Research Article **Open Access**

Abdelmadjid Abdi*, Khelifa Abbeche, Djamel Athmania, Mounir Bouassida

Effective Width Rule in the Analysis of Footing on Reinforced Sand Slope

https://doi.org/10.2478/sgem-2019-0005
received September 25, 2018; accepted January 28, 2019.

Abstract: This paper presents the results obtained from an experimental programme and numerical investigations conducted on model tests of strip footing resting on reinforced and unreinforced sand slopes. The study focused on the determination of ultimate bearing capacity of strip footing subjected to eccentric load located either towards or opposite to the slope facing. Strip footing models were tested under different eccentricities of vertical load. The obtained results from tests conducted on unreinforced sand slope showed that the increase in eccentricity of applied load towards the slope facing decreases the ultimate bearing capacity of footing. Predictions of the ultimate bearing capacity obtained by the effective width rule are in good agreement with those proposed from the consideration of total width of footing subjected to eccentric load. The ultimate bearing capacity of an eccentrically loaded footing on a reinforced sand slope can be derived from that of axially loaded footing resting on horizontal sand ground when adopting the effective width rule and the coefficient of reduction due to the slope. When increasing the distance between the footing border to the slope crest, for unreinforced and reinforced ground slope by geogrids, the ultimate bearing capacity of footing is no more affected by the slope ground.

Keywords: bearing capacity; eccentricity; footing; geogrid; model test; slope.

***Corresponding author: Abdelmadjid Abdi,** Department of Civil Engineering, Faculty of Technology University of Batna 2, Batna, Algeria, E-mail: a.abdi@univ-tebessa.dz
Khelifa Abbeche: Department of Civil Engineering, Faculty of Technology University of Batna 2, Batna, Algeria
Djamel Athmania: Department of Civil Engineering, University of Tebessa, Route de Constantine, 12002 Tébessa, Algeria
Mounir Bouassida: Université de Tunis El Manar, Ecole Nationale d'ingénieurs de Tunis, Ingénierie Géotechnique, LR14ES03, BP 37, Le Belvédère, 1002 Tunis, Tunisia

1 Introduction

Many types of shallow foundations can be designed when subjected to eccentric loading which depends on their geometrical shape or other influencing factors, as for footings located on slope ground. In this context, many researchers found that the ultimate bearing capacity of footings subjected to eccentric load on slope ground significantly decreases compared to those built on horizontal ground surface. This significant reduction is more likely attributed to load eccentricity and location of the footing with respect to the slope crest [1, 2]. The reduction in the ultimate bearing capacity due to the load eccentricity and/or the slope angle was studied by several investigators. Meyerhof [3] proposed a similar equation to that proposed by Terzaghi [4] by introducing the effective width of footing. According to this method, the ultimate load of a strip footing can be determined by assuming that the axial load is applied over the effective width of footing. Prakash and Saran [5] studied the bearing capacity of an eccentrically loaded footing on dense sand and on loose sand as well. Footings, of width B, were tested with zero embedding depth, D_f, i.e at ground surface and with embedment equals to footing width: $D_f/B = 1$. The load eccentricity was varied from $0.1B$ to $0.4B$. A reasonable agreement was found between the analytical results and measured model test results. Purkayastha and Char [6] studied, in detail, the problem of footing subjected to eccentric loads. The effective width introduced by Meyerhof was widely considered for the determination of the bearing capacity of eccentrically loaded footings. Michalowski and You [7] examined the validity of this method to estimate the bearing capacity of shallow foundations. The rule of effective width leads to suitable results to estimate the bearing capacity of eccentrically loaded footings and for any type of interface, between the footing and soil foundation, when the eccentricity is small, e.g. less than $0.15B$. Loukidis et al. [8] performed the finite element method to predict the ultimate bearing capacity of a footing resting on a purely frictional soil subjected to an eccentric load. This study led to the same finding when considering the effective width; the

reduction coefficient of bearing capacity depends on the internal friction angle. After numerous investigations on the stability of foundations built near a slope, it was shown that the ultimate load can be deduced from that of a foundation resting on horizontal ground by using a reduction coefficient which depends on the distance from the border of foundation to the slope crest and the slope angle. Meyerhof [2] reported that the bearing capacity of foundations near the crest slope decreases with the increase in the slope inclination. Beyond a distance of about six times the width of foundation, the bearing capacity does not depend on the inclination of the slope and becomes equal to that of a foundation resting on infinite horizontal ground surface. Gemperline [9] proposed an empirical coefficient of reduction for the determination of the bearing capacity of a footing on a cohesionless slope using the centrifuge test model. This coefficient depends on both the distance of the footing edge to the slope crest and the slope angle. This reduction coefficient permits to estimate the bearing capacity of foundations built near a slope ground. Garnier et al. [10] proposed a coefficient of reduction owed to the slope as identified from laboratory load test. Three inclinations of slope, characterized by horizontal to vertical distance: (H/V) = 3/2, 2/1 and 3/1, made up of sand having internal friction angle of 40.5° were tested. Recorded load failure allows the determination of the ratio of reduction in bearing capacity of the footing. This ratio considers the ultimate bearing capacity of a footing resting on sand slope and that of a footing on horizontal ground sand surface. Most of those studies focused on foundations subjected to eccentric loading or built on frictional soil slope. Reduction in the bearing capacity of the footing is due to the eccentricity and the slope angle. In turn, very few studies focused on the effects of bearing capacity reduction attributed to both the slope ground and the load eccentricity. Cure et al. [1] investigated a laboratory model test of strip footing subjected to axial and eccentric load. The experimental results were compared to analytical predictions based on the limit equilibrium approach and revealed in good agreement. Turker et al. [11] conducted a series of tests to investigate the ultimate bearing capacity of eccentrically loaded model footing resting on reinforced sand slopes. It was confirmed that the ultimate bearing capacity decreases when increasing the load eccentricity. This decrease in bearing capacity is due to load eccentricity and slope parameters. The use of geogrid reinforcement increased the ultimate bearing capacity in comparison to unreinforced ground.

Non-symmetrical failure surfaces were observed, primary failure surfaces developed on the slope side, and following failure surfaces developed on the opposite slope side. Lengths of failure surfaces decreased with increased eccentricity. The improvement of the bearing capacity of eccentrically loaded shallow foundations was the main objective of several investigations, especially when the reinforcing material is geotextile, e.g. Badakhshan and Noorzad [12], Patra et al. [13], Sahu et al. [14] and Saran et al. [15].

To date, the variation of ground slope subjected to eccentrically loaded footings was the most investigated. However, very few results are available in regard to the reinforcement effect by geogrids of ground slope.

In this paper, an experimental programme is detailed for studying the bearing capacity of strip footing subjected to eccentric load resting on ground slope made up of compacted sand. Experimental investigation also included the case of reinforced ground by geogrids. Numerical investigations, using the finite element code PLAXIS [16], are conducted to discuss the validity of effective width rule when estimating the ultimate bearing capacity of footing. Experimental and numerical results are interpreted to highlight the effects of variation of the load eccentricity, the distance between the footing and slope crest and the reinforcement by geogrid layers. Furthermore, the proposed results herein are compared to existing ones related to the coefficient of reduction in the ultimate bearing capacity owed to the combination of load eccentricity and inclination of slope ground.

2 Problem statement

Terzaghi's [4] work is the first referenced work where the formula given in Equation (1) was proposed to calculate the bearing capacity of strip footing:

$$q_{\mathrm{u}}=\frac{1}{2}B\gamma N_{\gamma}+CN_{\mathrm{C}}+qN_{\mathrm{q}} \tag{1}$$

q_{u} denotes the ultimate bearing capacity of footing of width B subjected to vertical and axial load, γ is the unit weight of soil foundation of cohesion C and internal friction angle φ, $(N_{\gamma}, N_{\mathrm{c}}, N_{\mathrm{q}})$ are the bearing capacity factors which only depend on the soil friction angle.

"q" is the vertical uniform surcharge applied at ground surface around the footing.

To account for the load eccentricity "e", Meyerhof [3] proposed Equation (2), which is identical to Equation (1) by Terzaghi [4]:

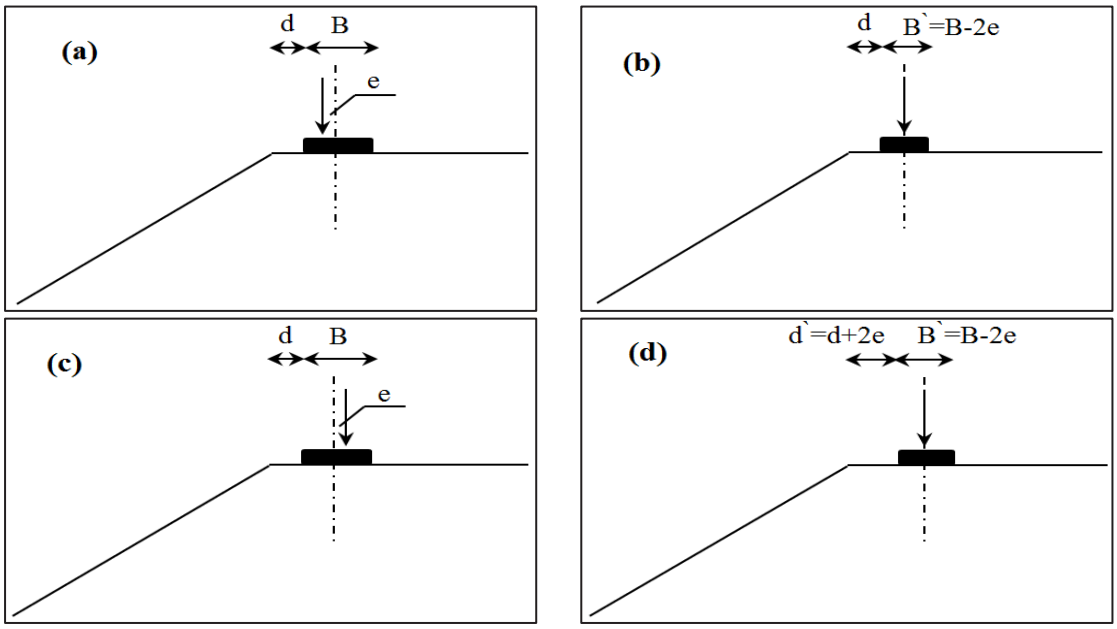

Figure 1: Schematic view of footing model considering the effective width of footing.

$$q_{ue}=\frac{1}{2}B'\gamma N_{\gamma}+CN_{C}+qN_{q} \quad (2)$$

q_{ue} is the ultimate bearing capacity of eccentrically loaded footing $B'=B\left(1-\frac{2e}{B}\right)$ is the effective width of footing; e is the load eccentricity with respect to the geometrical axis of the footing (Fig. 1a).

The rule of effective width is herein adopted to estimate the bearing capacity of an eccentrically loaded strip footing on reinforced sand slope. Two cases of load eccentricity are investigated. The first case corresponds to the load eccentricity oriented towards the slope facing (Fig. 1b); in the second case, the load eccentricity is located opposite to the slope facing (Fig. 1c). Accordingly, two cases of eccentricity are modelled as a footing having an effective width subjected to centred load with two different distances from the slope crest. The first distance accounts for the case of eccentrically loaded footing located towards the slope facing, and it is equal to the same distance for an eccentrically loaded footing with a total width "*d*" (Fig. 1a and b). The second distance accounts for the case of an eccentrically loaded footing opposite to the slope facing, and it is equal to the distance for an eccentrically loaded footing with a total width *d* plus two times the load eccentricity, *d*' = *d* + 2*e* (Fig. 1c and d).

3 Experimental study

3.1 Setup of the experimental model

A scaled strip footing model was built within a rigid steel box of dimensions 1.5 m ´ 0.5 m in plane and 0.6 m in height. One side of the rigid box was built of thick and transparent glass to visualize the installation of each sand layer during the construction of ground slope. Rigid box walls are made up of melted steel to minimize the friction with footing borders. This plane strain model is used to examine the effect of eccentric loads on the bearing capacity of strip footing. Loading tests were conducted on unique model slope β: $tg(\beta) = 0.67$.

Detailed description of the model test apparatus is shown in Fig. 2a. The loading device comprises a moving lever mechanism equipped with a rigid metal beam. Applied load on the footing results from cumulating masses placed on the lever (proving ring of 20 kN capacity). The displacements were measured by a sensor placed on the contact load point as shown in Fig. 2b. A schematic view of the test model with notations used in this study is shown in Fig. 3.

The footing length is equal to the width of rigid box. Footing endings have been lubricated to eliminate the frictional contact with the rigid box borders. The dimensions of the footing are 498 mm ´ 100 mm in plane and 20 mm in thickness. Several holes were created on the upper side of the footing to enable different eccentricities

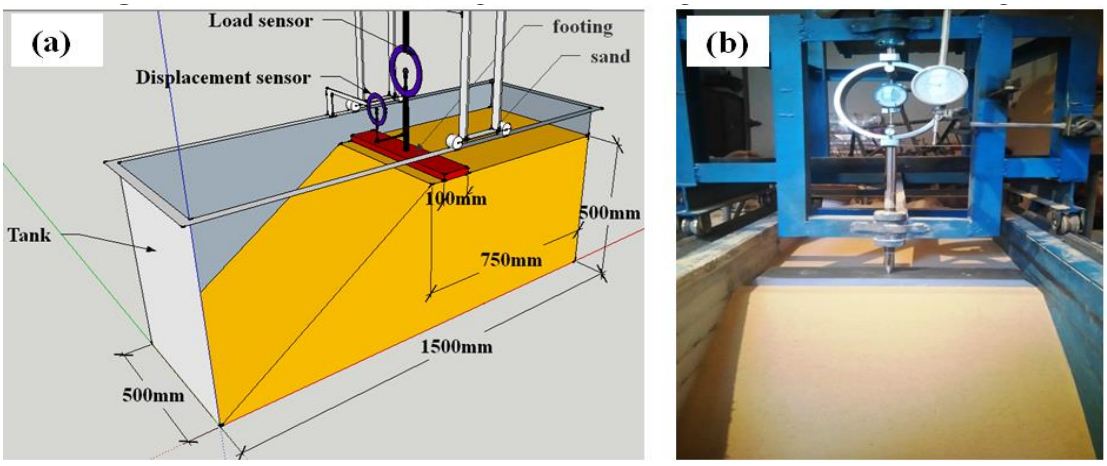

Figure 2: Laboratory model test.

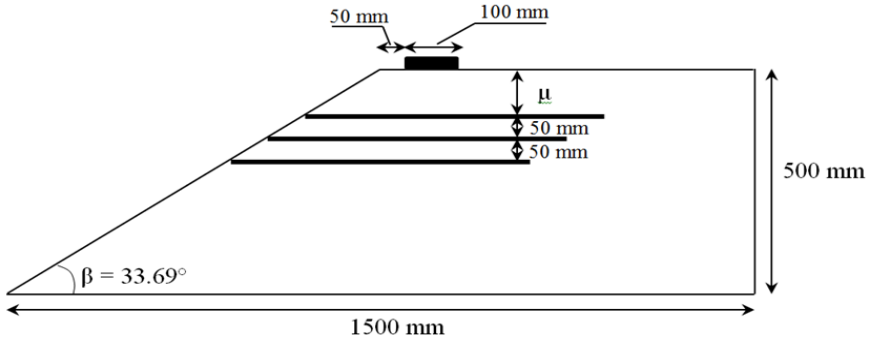

Figure 3: Cross section of model test in the case of reinforced ground by geotextiles.

of the applied load. The footing is allowed to rotate freely at the point of applied load. The footing roughness is assured by glued sand paper layer. The strip footing model with a series of holes is shown in Figs. 2b and 4.

Figure 4: Tested footing with location of applied load.

3.2 Test materials

3.2.1 Sand

The tested sand was extracted from the region of Tébessa located in South-East Algeria. The dry unit weight of tested sand varies from 13.75 to 19.1 kN/m^3, from the grain size distribution as shown in Fig. 5; it is a coarse sand having coefficient of uniformity: C_u = 4.28 and the coefficient of curvature is C_c = 1.85. For all performed tests, the sand was dried up to zero moisture content. The rigid box was filled by sand following the steps of pouring compaction technique of thin sub-layers of 5 cm thickness formed by homogeneous compacted soil.

The construction of reinforced soil models was carefully controlled during the setup of experimental model to assure a uniform soil density, which corresponds to relative density of approximately 60%, and the dry unit weight of 16.1 kN/m^3 was obtained. The measured internal friction angle of compacted coarse sand at relative density equals 60%, from a series of direct shear tests, was approximately 41°. Other geotechnical parameters of the tested sand are summarized in Table 1.

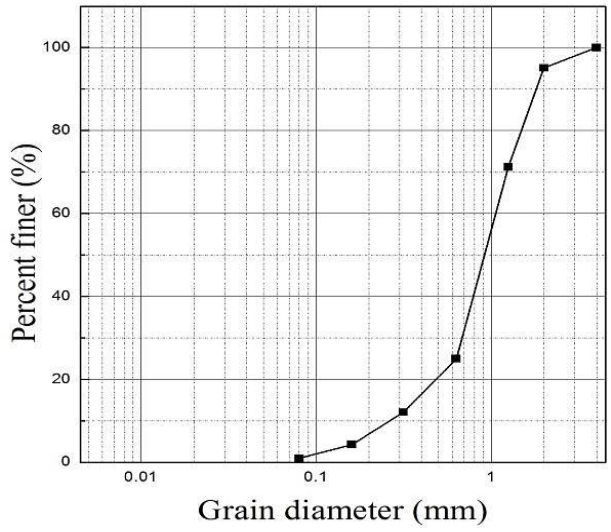

Figure 5: Grain size distribution of tested sand.

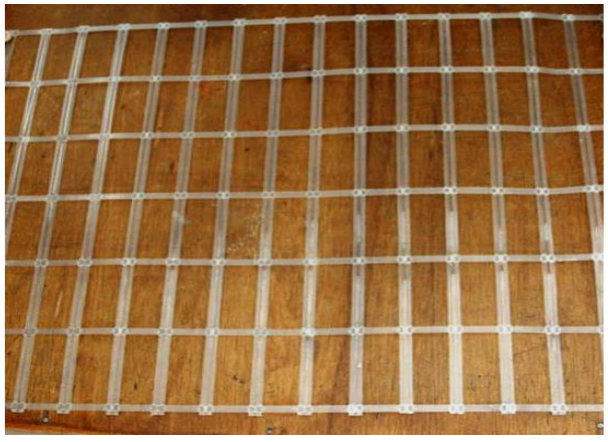

Figure 6: View of geogrid reinforcement.

Table 1: *Material properties of the sand used.*

Parameters	Values
Cohesion, c (kPa)	0.0
Angle of internal friction (°)	41
Dry unit weight (kN/m^3)	16.1
Maximum dry density (kN/m^3)	19.1
Minimum dry density (kN/m^3)	13.75
D_{10}	0.28
D_{60}	1.20
D_{30}	0.79
Coefficient of uniformity, C_u	4.28
Coefficient of curvature, C_c	1.85

Table 2: *Geogrid properties.*

Description	R6 80/20
Raw material	Transparent polyester
Surface ground (g/m^2)	380
Tensile strength (kN/m)	$20 \le R_T \le 80$
Elongation (%)	$0 \le \Delta L \le 8$
Tensile strength for 1% elongation (kN/m)	16
Tensile strength for 2% elongation (kN/m)	28
Tensile strength for 5% elongation (kN/m)	56
Meshes opening (mm ´ mm)	73 ´ 30
Elongation before service (%)	0
Roller dimensions, length and width (m ´ m)	4.75 ´ 100

3.2.2 Reinforcements

The reinforcing geogrid type tested in the carried out experiments is *R*6 80/20 made up of high-density polyethylene (Fig. 6). Characteristics of this reinforcement are as follows: mesh aperture size of 30 mm ´ 73 mm; maximum tensile strength = 56 kN/m. Remaining properties of the geogrid are given in Table 2.

3.3 Slope preparation and experimental programme

For the construction of reinforced ground slope, the experimental procedure described by Lee and Manjunath [17] was adopted. The slope of the sand is prepared so that it provides a slope angle of 33.69°. The sand is poured and compacted by horizontal sub-layers of 50 mm thickness. The geogrid layer is placed on levelled compacted surface at desired depth. The sand-filling procedure was pursued layer by layer until total height was reached. Then, according to the geometry of the slope drawn on both sides of the rigid box, the compacted sand was smoothly excavated. The slope facing was levelled using a rigid metal blade for the desired inclination. The length (L) of reinforcing geogrid was kept constant for all reinforced layers; the installation of geogrid ended at the slope facing. The footing was then placed on the ground surface at distance d = 50 mm from the slope crest. Three series of tests were conducted to analyze the effect of eccentrically loaded footing on the slope behaviour. The loading of three series of tests is as follows: (1) centred vertical load; (2) an eccentric load when the load eccentricity is

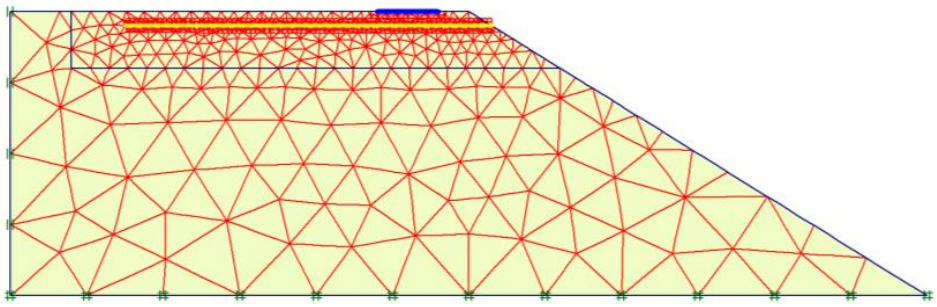

Figure 7: Geometry and mesh size of the numerical model.

towards the slope (Fig. 1a); (3) an eccentric load when the load eccentricity is opposite to the slope (Fig. 1c). Each series of tests consisted in studying the response of given parameter, whilst other ones were kept constant. The varied conditions included the eccentricity value, the number of geogrid layers (N) and the depth of the first geogrid layer below the ground surface (μ). Table 3 summarizes the experimental programme conducted on geogrid-reinforced slopes with following notations:

"e/B" denotes the normalized eccentricity;
"d/B" denotes the normalized distance of applied load;
"μ/B" denotes the normalized depth of geogrid reinforcement.
"N" denotes the number of geogrid layers

In Table 3, the notation "C" refers to centred load, "T" refers to eccentricity values towards the slope and "F" refers to eccentricity values opposite to the slope.

Table 3: *Parameters and conditions of performed tests.*

Test reference	N	μ/B	e/B	d/B
C0	0		0	0.5
T01, F01			0.1	
T02, F02			0.2	
T03, F03			0.3	
C250	1	0.25	0	
T251, F251			0.1	
T252, F252			0.2	
T253, F253			0.3	
C500		0.5	0	
T501, F501			0.1	
T502, F502			0.2	
T503, F503			0.3	
C750		0.75	0	
T751, F751			0.1	
T752, F752			0.2	
T753, F753			0.3	

4 Numerical study

The assessment of numerical predictions is carried out by the experimental results obtained from the current study.

4.1 The numerical model

The numerical analysis was carried out by using the finite element PLAXIS code [16] which provides solutions to several geotechnical problems. A two-dimensional finite element analysis (FEA) on a slope ground model is carried out to evaluate the ultimate load and to predict the deformations in the sand ground subjected to eccentrically loaded foundation. The initial conditions included the state of initial effective stress of dry sand. The geometry of numerical model was adopted the same as for the laboratory model. Also, the same material properties (footing, geogrid and sand) were adopted as for the tested model.

Figure 7 shows the geometry of typical model for the numerical analysis. The boundary conditions comprise constrained horizontal displacement along lateral borders, and vertical and horizontal displacements are zero at the bottom of numerical model.

For the reinforced ground, the reinforcing layers were placed at the desired depth, and the suitable strength reduction factors between the contact surfaces and the stiffness of geogrid were the added input parameters.

These parameters were introduced in the interface menu of PLAXIS software. The refined mesh option was

Table 4: *Parameters used in the numerical study.*

Material	γ_{unsat} (kN/m³)	γ_{sat} (kN/m³)	E (kn)	ν	EA (kPa)	EI (kN.m²)	φ(°)	ψ(°)	R
Sand	16.1	19.12	14,000	0.3	–	–	41	8	0.7
Geogrid		–	–	–	500	–	–	–	–
Foundation	–	–	–	–	2.10E+07	1.75E+03	–	–	–
	–								

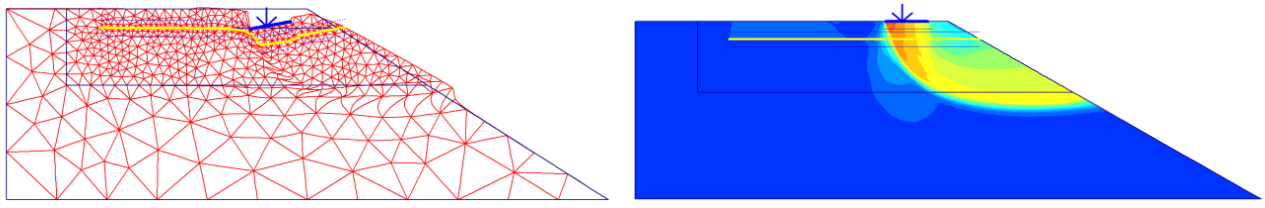

(a) Deformed mesh (b) Contours of total displacement

Figure 8: Outputs of PLAXIS code for $e/B = 0.1$ opposite to the slope facing. (a) Deformed mesh; (b) contours of total displacement.

adopted to reduce the effect of mesh dependency when analyzing the model parameters (i.e. the location of geogrid layers and variation of loaded area). The initial stress condition of the slope was generated by the gravity force characterized by soil unit weight including the geogrid reinforcements.

4.2 Finite element modelling

Several numerical models were carried out by adopting the Mohr–Coulomb constitutive law for the sand slope due to its simplicity and easy determination of soil parameters. For the reinforced sand, the interaction between geogrid and soil is modelled by interface elements on both top and bottom sides of the geogrid. The adopted parameters of numerical analysis are summarized in Table 4.

5 Results and discussion

Twenty-seven experimental models were built to carry out loading tests, up to failure, on centrally and eccentrically loaded strip footings in both unreinforced and reinforced ground slope. The ultimate load is determined from the load settlement curves by using the tangent intersection method proposed by Trautmann and Kulhawy [18]. Two tangent lines are drawn at the initial and final points of the curve; the intersection point of those tangents represents the ultimate load of the tested foundation. The obtained experimental results are summarized in Tables 5 and 6. Discussion of those results is suggested for two cases of load eccentricity and varied distance between the applied load and the crest slope.

Figures 8 and 9 show the outputs of PLAXIS code comprising the deformed meshes (Figs 8a and 9a) and the contours of total displacements (Figs 8b and 9b). The studied case refers to eccentric (e = 0.1 B) on reinforced sand slope by one geogrid layer. From those curves, the effect of eccentricity is evaluated by the maximum total displacement under the footing which is equal to 2.64 and 1.75 mm for eccentricities towards and opposite to the slope facing, respectively. This result explains why the eccentric load when the applied load opposite to the facing of slope provides a better behaviour of the footing by lesser displacement than that predicted for load applied towards the slope facing.

5.1 Load eccentricity located towards the slope facing

Figure 10 illustrates the experimental results of model footing tested under varied eccentricities located towards the slope facing. As shown in Fig. 10, the ultimate bearing capacity decreases when the eccentricity of applied load increases. This trend confirms the experimental results proposed by Patra et al. [13] and Turker et al. [11].

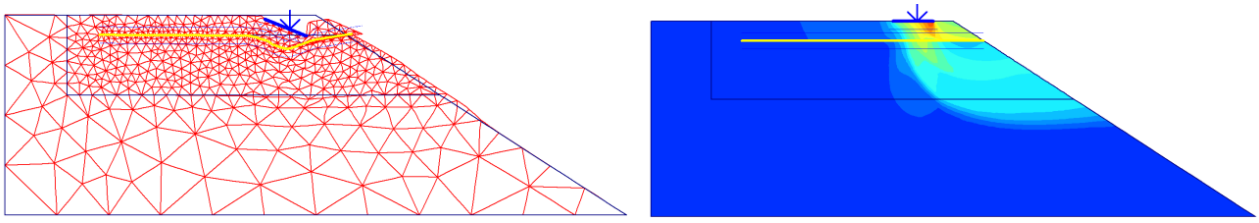

Figure 9: Outputs of PLAXIS code for $e/B = 0.1$ towards the slope facing. (a) Deformed mesh; (b) contours of total displacement.

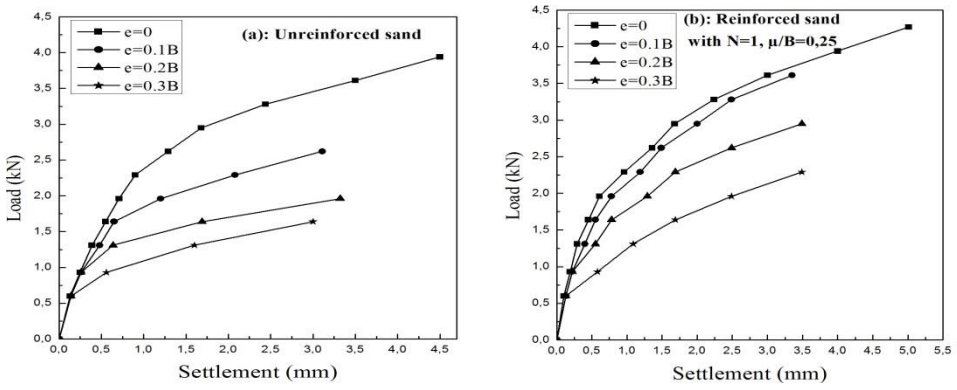

Figure 10: Relationship between the failure load and the displacements of a strip footing under various eccentricities located towards the reinforced slope face.

Table 5: *Ultimate loads of footing under various load eccentricities located towards the slope face.*

N	μ/B	e/B	q_u (kN/ml)			i_B; total width	i_B; effective width
			Experimental results	Numerical results using total width method	Numerical results using effective width method		
0		0	2.71	2.81	2.81	1.000	1.000
		0.1	1.78	1.96	2.02	0.698	0.719
		0.2	1.38	1.5	1.54	0.534	0.548
		0.3	0.98	1.06	1.11	0.377	0.395
1	0.25	0	2.81	3.13	3.13	1.000	1.000
		0.1	2.53	2.66	2.75	0.850	0.879
		0.2	1.93	2.06	2.08	0.658	0.665
		0.3	1.22	1.32	1.45	0.422	0.463
		0.4		0.64	0.66	0.204	0.211
	0.5	0	3.08	3.18	3.18	1.000	1.000
		0.1	2.61	2.76	2.81	0.868	0.884
		0.2	1.78	1.88	1.91	0.591	0.601
		0.3	0.95	1.06	1.11	0.333	0.349
	0.75	0	3.11	3.2	3.2	1.000	1.000
		0.1	2.24	2.42	2.55	0.756	0.797
		0.2	1.53	1.42	1.52	0.444	0.475
		0.3	0.88	0.97	1.02	0.303	0.319

Table 6: *Ultimate loads of footing under various load eccentricities located opposite to the slope face.*

N	μ/B	e/B	q_u (kN/ml)			i_B; total width	i_B; effective width
			Experimental results	Numerical results with total width method	Numerical results with effective width method		
0		0	2.71	2.81	2.81	1.000	1.000
		0.1	2.33	2.46	2.51	0.875	0.893
		0.2	2.08	2.02	2.1	0.719	0.747
		0.3	1.54	1.61	1.7	0.573	0.605
1	0.25	0	2.81	3.13	3.13	1.000	1.000
		0.1	2.55	2.7	2.83	0.863	0.904
		0.2	2.21	2.36	2.44	0.754	0.780
		0.3	1.61	1.82	1.93	0.581	0.617
	0.5	0	3.08	3.18	3.18	1.000	1.000
		0.1	3	3.16	3.22	0.994	1.013
		0.2	2.75	2.87	2.96	0.903	0.931
		0.3	1.98	2.1	2.15	0.660	0.676
	0.75	0	3.11	3.2	3.2	1.000	1.000
		0.1	3.1	3.23	3.27	1.009	1.022
		0.2	2.52	2.66	2.71	0.831	0.847
		0.3	1.28	1.39	1.48	0.434	0.463

The numerical analysis aims to check the use of effective width assumption on the value of ultimate bearing capacity of eccentrically loaded footing when the load eccentricity is oriented towards the slope facing. The strip footing, located at the same distance as for a centrally loaded footing d, is assumed having an effective width B. The coefficient of reduction in the ultimate bearing capacity of footing is characterized by a non-dimensional coefficient i_B. This coefficient of reduction in the ultimate bearing capacity of an eccentrically loaded strip footing (q_{uecc}) with respect to the ultimate bearing capacity of the same footing subjected to central vertical load (q_{uc}) is:

$$i_B = \frac{q_{u\ eccenric}}{q_{u\ centric}} \tag{3}$$

Figure 11 displays the load settlement curves of eccentrically loaded footing on unreinforced and reinforced sand slope with one geogrid layer located at depth defined as m/B = 0.25. First, it is well shown that all curves in Fig. 11 have a unique trend. Second, it is seen that the more is the eccentricity of applied load and the less is the first linear portion of the load settlement curves, and, consequently, the ultimate bearing capacity of footing decreases.

Figure 12 shows the variation of coefficient of reduction in the ultimate bearing capacity i_B versus the eccentricity ratio e/B of an eccentrically loaded footing with an eccentricity located towards the slope facing for unreinforced and reinforced ground slope.

As can be seen, the results of an eccentrically loaded footing using the effective width are almost identical to those obtained for an eccentrically loaded footing with total width for both cases of unreinforced and reinforced sand slope. This finding can be argued by the fact that the slope behaved in similar way for two tested footings, because the distance from the footing edge to the slope crest was kept unchanged. The portion of the footing that carried the load remains the same which implies that the combination of the load eccentricity and the slope by using the effective width rule can lead to good results. Loukidis et al. [8] reported that using the Meyerhof's [3] effective width $B'=B-2e$, one can capture that the effect of the load eccentricity and load inclination is combined. In this study, the effective width $B'=B-2e$ can also express the effect of the load eccentricity for the case of a load eccentricity–slope combination. The ultimate bearing capacity of an eccentrically loaded footing near a reinforced or unreinforced sand slope may be derived

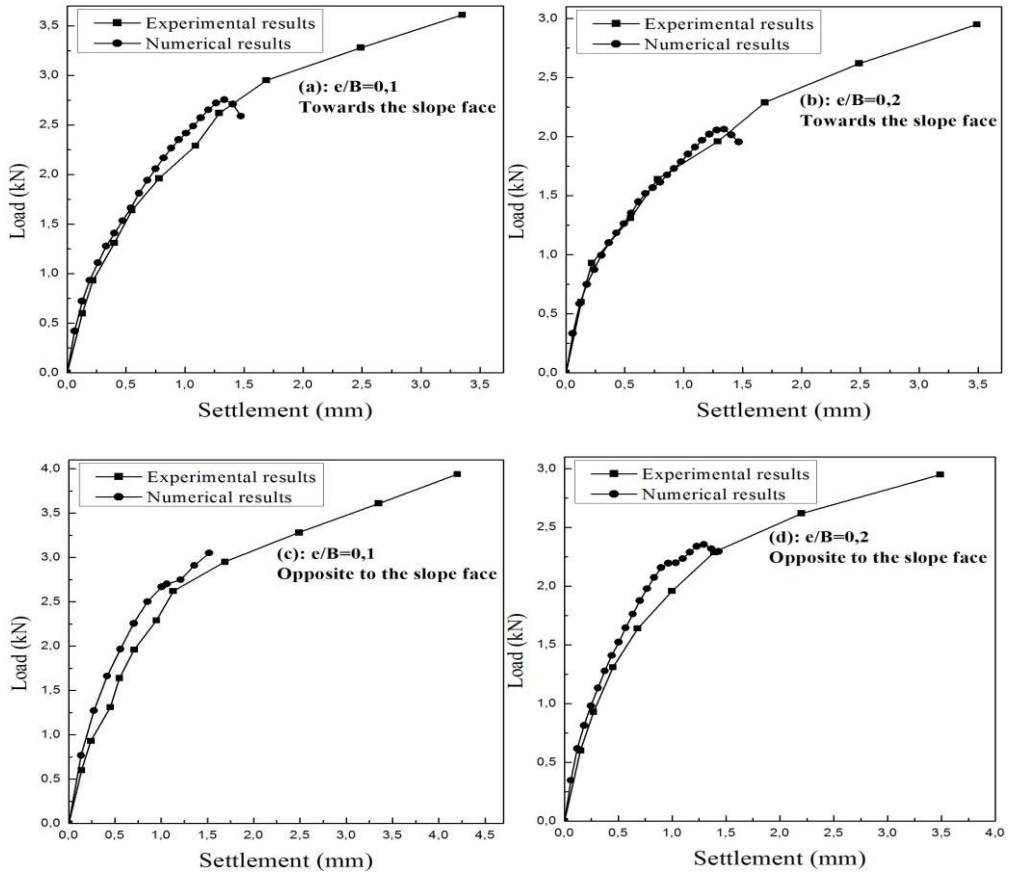

Figure 11: Comparison between the experimental and numerical results for reinforced sand ($N = 1$, $m/B = 0.25$).

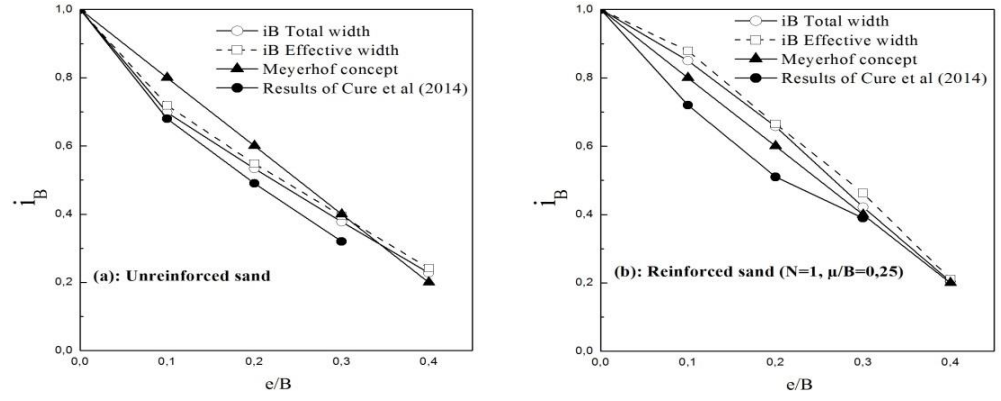

Figure 12: Variation of i_B versus e/B of a strip footing under eccentric load located towards the reinforced slope face.

from that of a footing resting on horizontal ground using two reduction coefficients linked to the load eccentricity $i_e = 1-(2e/B)$ and to the slope subjected to a footing of reduced width $B' = B - 2e$ located at distance d with respect to the slope crest. In Figs 11a and b a comparison can be made between the proposed results in this paper and those given by Turker et al. [11] and Meyerhof's [3] rule for unreinforced soil. It is clear that the predictions when adopting the rule of effective width agree with the proposed results in literature for both cases of unreinforced and reinforced slope ground.

In the case of a strip footing located near a sand slope reinforced by geogrids and subjected to an eccentric load located towards the slope facing, the ultimate load can be expressed by the formula in Equation (4):

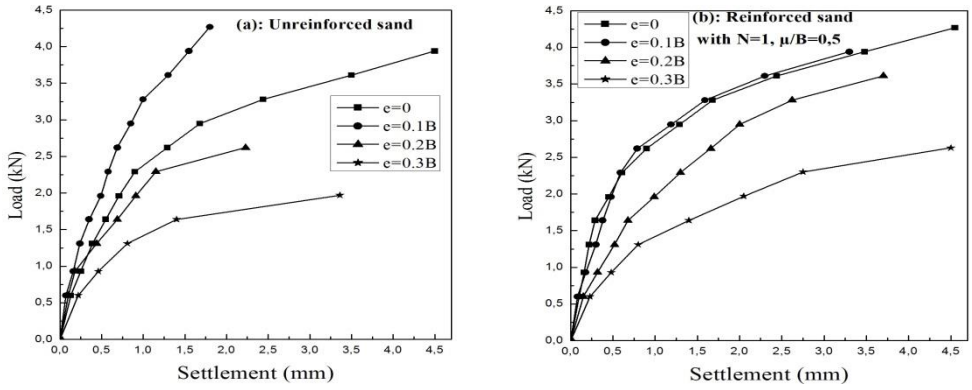

Figure 13: Relationship between the failure load and the displacements of a strip footing under various eccentricities located opposite to the reinforced slope face.

$$q_{uesB} = q_{uch\,B} \times i_{\beta(d,B)} \quad (4)$$

$q_{ues\,B}$ is the ultimate bearing capacity of an eccentrically loaded strip footing with total width resting near sand slope, $q_{uch}B$ is the ultimate bearing capacity of a centrally loaded strip footing with effective width resting on horizontal ground.

$i_{\beta(d,\,B')}$ is the reduction coefficient due to the slope as a function of the distance between the border of footing and the slope crest, the effective width and the load eccentricity (Fig. 1b).

5.2 Load eccentricity located opposite to the slope facing

Figure 13a and b illustrates the test results of model footing subjected to various eccentricities opposite to the slope facing. As shown in Fig. 13a, it is clear that the ultimate bearing capacity of footing on unreinforced ground slope decreases when the eccentricity of applied load increases. As shown in Fig. 13b, the ultimate bearing capacity of footing is not affected by the load eccentricity in the range of $e \leq 0.1$ m. In fact, the variation of applied eccentric load versus settlement coincides with that of vertical central load (zero eccentricity). Such observation can be explained by the fact that the inclination effect is balanced by the increase in the length of reinforcing geogrid against sliding due to the increase in distance between the applied load and the slope crest. This also proves that in case the load eccentricity is located opposite to the slope facing, the ultimate bearing capacity is greater than that corresponding to the eccentric load located towards the slope facing. Figure 14 shows the variation of i_B ratio versus e/B ratio of footing subjected to an eccentric load located opposite to the slope facing for unreinforced and reinforced sand slopes. As for the case of load eccentricity oriented towards the slope facing, the use of effective width rule leads to acceptable results which are quite comparable to those obtained in case of an eccentrically loaded footing considered with total width. Figure 14a and b compares between the results of current study and those proposed by Turker et al. [11] and the Meyerhof's rule [3] for unreinforced sand slope. In this case when the load eccentricity is located opposite to the slope facing, it is well noted that proposed results herein exceed the predictions by the Meyerhof's concept. This exceedance can be explained by the fact that the distance between the footing border and the slope crest is greater to that when the load eccentricity is located towards the slope facing. As shown in Fig. 1d, the footing was numerically modelled with an effective width $B = B\text{-}2e$ and located at a distance from the slope crest $d' = d + 2e$. For the reinforced sand slope as shown in Fig. 14b, there is a discrepancy between the results of the present study and those presented by Turker et al. [11] and Meyerhof's rule [3]. This discrepancy is likely linked to the failure mechanism corresponding to loaded footing on slope ground. The observed behaviour from the load settlement curve and the type of failure mechanism of reinforced slope are significantly affected by the geogrid reinforcement located at a specific depth [19–21].

When the load eccentricity is located opposite to the slope facing, the ultimate bearing capacity can be expressed by Equation (5):

$$q_{uesB} = q_{uch\,B} \times i_{\beta(d,B)} \quad (5)$$

$i_{\beta(d',\,B')}$ is the reduction coefficient due to the slope as a function of distance: $d' = d + 2e$ and the effective width.

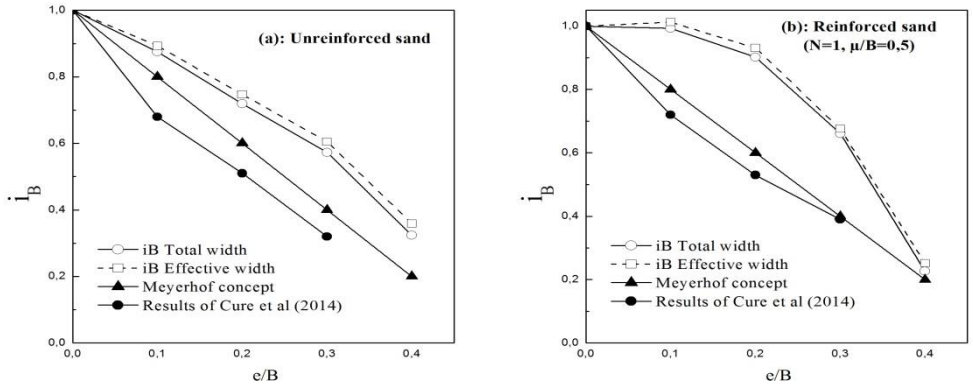

Figure 14: Variation of i_B versus e/B of a strip footing under load eccentricity located opposite to the reinforced slope face.

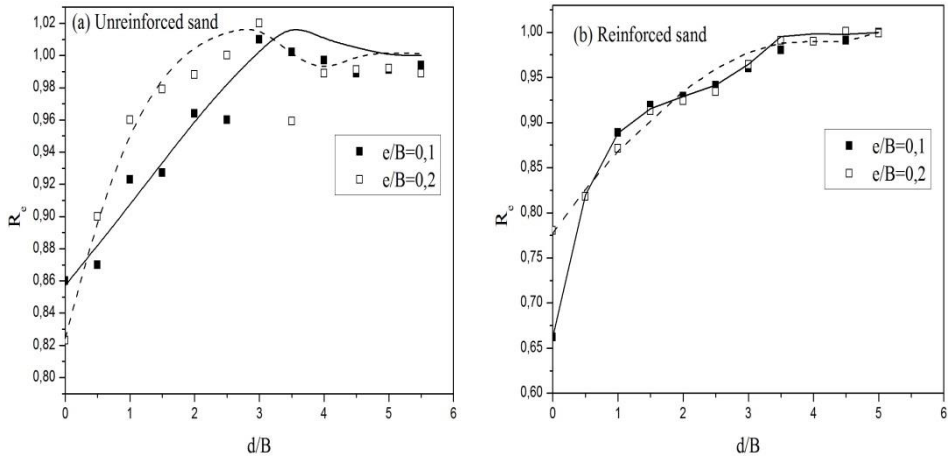

Figure 15: Variation of R_e versus d/B.

5.3 Effect of the distance between the footing border and the slope crest

The location of footing is characterized by the distance between the crest slope of sand ground and the border of footing. The influence of this distance on the ultimate bearing capacity of eccentrically loaded strip footing either towards or opposite to the facing of slope ground is studied below. Hence, in terms of normalized parameters one introduces:

The ratio, denoted by $R_{e,}$ which corresponds to the ultimate bearing capacity of a footing subjected to an eccentric load, located towards the slope facing, to that of a footing subjected to an eccentric load located opposite to the slope facing.

The ratio "d/B" is the normalized distance between the crest of slope ground and the border of footing.

Figure 15 shows the variation of R_e versus the ratio (d/B) for the unreinforced and reinforced ground sand slopes for two normalized load eccentricities $e/B = 0.1$ and $e/B = 0.2$.

In the case of unreinforced soil, as shown in Fig. 15a, it can be seen that values of R_e ratio, for a strip footing located over the distance equals $3B$, are 0.98 and 1.2, respectively. This indicates that the ultimate bearing capacity of an eccentrically loaded footing located at a distance larger than $3B$ (eccentricity is located towards the slope facing) is quite close that obtained for load eccentricity located opposite to the slope facing.

Figure 15b shows (for reinforced ground slope) that the obtained values of the R_e ratio for strip footing located at the distance $3.5B$ are 0.98 and 0.97, respectively. It is concluded that there would be no benefit in moving the footing any further from the slope crest. Meanwhile, in case the load eccentricity is located opposite to the slope facing, the ultimate bearing capacity is greater to that obtained for the case where the load eccentricity is located towards the slope facing. This increase in the ultimate

bearing capacity becomes higher in the case of reinforced ground slope.

The reinforcing effect increases by increasing the distance between the location of applied load and the slope crest. Therefore, for the case of reinforced sand, a third parameter should be introduced to take into account the reinforcement effect. This parameter depends on the load eccentricity and the reinforcement effect.

Hence, Equation (5) is transformed as follows:

$$q_{\mathrm{ues}B} = q_{\mathrm{uch}\,B} \times i_{\beta(d,B)} \times C_{\mathrm{R}} \tag{6}$$

C_{R} is the coefficient which takes into account the reinforcement effect. This coefficient can be deduced from the comparison of measured ultimate bearing capacity of strip footing subjected to eccentric load built on unreinforced and reinforced ground slope.

6 Conclusions

In this paper, the determination of ultimate bearing capacity of strip footing built on unreinforced and reinforced ground sand slope was investigated. Three parameters were considered in the framework of plane strain analysis to study the variation of ultimate bearing capacity of strip footing either measured from load test laboratory models or predicted from numerical calculation.

The eccentricity of vertical load subjected to the footing was the first parameter to be investigated for two configurations; eccentricity towards the slope facing or eccentricity opposite to the slope facing. The distance between the border of footing and the crest of slope was the second parameter of influence. The third parameter is related to the reinforcement of sand slope by geogrid layers. Main findings from experimental and numerical results presented in this paper are summarized as follows.

The consideration of the effective width rule for the determination of ultimate load of an eccentrically loaded strip footing located near a reinforced sand slope, leads to comparable results previously suggested for a footing with a total width.

The ultimate load of an eccentrically loaded footing on a reinforced sand slope can be derived from that of axially loaded footing resting on the horizontal reinforced sand ground by introducing the two coefficients of reduction due to the load eccentricity i_{e} and to the slope inclination i_{β}.

In the case of reinforced sand slope, when the load eccentricity is located opposite to the slope facing, a third parameter must be introduced to take into account the reinforcing effect. This parameter is related to the load eccentricity and the reinforcement parameters.

Beyond a distance from the slope crest equals three times the width of footing, the ultimate bearing capacity is insignificantly affected by the location of applied load, i.e. towards the slope facing or opposite to it.

References

[1] Cure, E., Turker, E., Uzuner, B.A. (2014). Analytical and experimental study for ultimate loads of eccentrically loaded model strip footings near a sand slope. *Ocean Engineering, 89*, 113-118. doi: 10.1016/j.oceaneng.2014.07.018.

[2] Meyerhof, G. (1957). The ultimate bearing capacity of foundations on slopes. In: *Proc., 4th Int. Conf. on Soil Mechanics and Foundation Engineering*.

[3] Meyerhof, G. (1953). The bearing capacity of foundations under eccentric and inclined loads. In: *Proc. of 3rd ICSMFE*.

[4] Terzaghi, K. (1943). Bearing capacity. *Theoretical Soil Mechanics*, 118-143. doi: 10.1002/9780470172766.ch8.

[5] Prakash, S., Saran, S. (1971). Bearing capacity of eccentrically loaded footings. *Journal of Soil Mechanics and Foundations Division*.

[6] Purkayastha, R.D., Char, A. (1977). Stability analysis for eccentrically loaded footings. *Journal of Geotechnical and Geoenvironmental Engineering, 103*, GT-6, 647-651. http://ojps.aip.org/gto

[7] Michalowski, R.L., You, L. (1998). Effective width rule in calculations of bearing capacity of shallow footings. *Computers and Geotechnics, 23*(4), 237-253. doi: 10.1016/S0266-352X(98)00024-X.

[8] Loukidis, D., Chakraborty, T., Salgado, R. (2008). Bearing capacity of strip footings on purely frictional soil under eccentric and inclined loads. *Canadian Geotechnical Journal, 45*(6), 768-787. doi: 10.1139/T08-015.

[9] Gemperline, M.C. (1988). Centrifugal modeling of shallow foundations. *Soil Properties Evaluation from Centrifugal Models and Field Performance*.

[10] Garnier, J., Canepa, Y., Corte, J., Bakir, N. (1994). Study of bearing capacity of footings near slopes. In: *Proc. of Int. Conf. on Soil Mechanics and Foundation Engineering -ISSMFE, New Delhi January 1994*.

[11] Turker, E., Sadoglu, E., Cure, E., Uzuner, B.A. (2014). Bearing capacity of eccentrically loaded strip footings close to geotextile-reinforced sand slope. *Canadian Geotechnical Journal, 51*(8), 884-895. doi: 10.1139/cgj-2014-0055.

[12] Badakhshan, E., Noorzad, A. (2015). Load eccentricity effects on behavior of circular footings reinforced with geogrid sheets. *Journal of Rock Mechanics and Geotechnical Engineering, 7*(6), 691-699. doi: 10.1016/j.jrmge.2015.08.006.

[13] Patra, C., Das, B., Bhoi, M., Shin, E. (2006). Eccentrically loaded strip foundation on geogrid-reinforced sand.

Geotextiles and Geomembranes, 24(4), 254-259. doi: 10.1016/j.geotexmem.2005.12.001.

[14] Sahu, R., Patra, C., Das, B., Sivakugan, N. (2016). Ultimate bearing capacity of rectangular foundation on geogrid-reinforced sand under eccentric load. *International Journal of Geotechnical Engineering, 10*(1), 52-56. doi: 10.1179/1939787915Y.0000000008.

[15] Saran, S., Kumar, S., Garg, K., Kumar, A. (2007). Analysis of square and rectangular footings subjected to eccentric-inclined load resting on reinforced sand. *Geotechnical and Geological Engineering, 25*(1), 123-137. doi: 10.1007/s10706-006-0010-7.

[16] Brinkgreve, R. (2002). *Plaxis: Finite Element Code for Soil and Rock Analyses: 2D-Version 8:[User's Guide]*. Balkema.

[17] Lee, K., Manjunath, V. (2000). Experimental and numerical studies of geosynthetic-reinforced sand slopes loaded with a footing. *Canadian Geotechnical Journal, 37*(4), 828-842. doi: 10.1139/t00-016.

[18] Trautmann, C.H., Kulhawy, F.H. (1988). Uplift load-displacement behavior of spread foundations. *Journal of Geotechnical Engineering, 114*(2), 168-184. doi: 10.1061/(ASCE)0733-9410(1988)114:2(168).

[19] El Sawwaf, M. (2009). Experimental and numerical study of eccentrically loaded strip footings resting on reinforced sand. *Journal of Geotechnical and Geoenvironmental Engineering, 135*(10), 1509-1518. doi: 10.1061/(ASCE)GT.1943-5606.0000093.

[20] Huang, C.-C., Tatsuoka, F., Sato, Y. (1994). Failure mechanisms of reinforced sand slopes loaded with a footing. *Soils and Foundations, 34*(2), 27-40. doi: 10.3208/sandf1972.34.2_27.

[21] Huang, C., Tatsuoka, F. (1994). Stability analysis for footings on reinforced sand slopes. *Soils and Foundations, 34*(3), 21-37. doi: 10.3208/sandf1972.34.2_27.